Magnetopolaron effect in parabolic quantum wells in tilted magnetic fields

G.-Q. Hai
Instituto de Física de São Carlos, Universidade de São Paulo, 13560-970, São Carlos, SP, Brazil

F. M. Peeters
Departement Natuurkunde, Universiteit Antwerpen (UIA), B-2610 Antwerpen, Belgium

(Received 19 January 1999)

The magnetopolaron is investigated in parabolic quantum wells in the presence of a tilted magnetic field. The Landau levels of polarons in GaAs/$Ga_{1-x}Al_xAs$ parabolic quantum wells are calculated for different subbands. The effect of the electron-phonon interaction on the polaron energy levels is included within second-order perturbation theory. The influence of the direction of the magnetic field on the polaron effect on the different electron energy levels is studied. Possible magnetopolaron resonances are also discussed.
[S0163-1829(99)02132-3]

I. INTRODUCTION

In recent years, improvements of the semiconductor growth techniques have offered the possibility to obtain low-dimensional semiconductor structures with any desired well shapes. One of those structures is the so-called parabolic quantum well (PQW). The PQW's based on GaAs have been developed by tailoring the conduction-band edge of a graded $Ga_{1-x}Al_xAs$ semiconductor by properly varying the Al mol fraction x.[1–3] Remotely doped wide PQW's have been proposed as structures in which a high mobility quasi-three-dimensional electron gas can be realized. Magnetotransport experiments on these systems confirmed the existence of a thick slab of high mobility electron gas. Such structures are closely related to the theoretical construction of jellium, consisting of a highly mobile dilute electron gas in the potential of a positively charged background. Interestingly, in these systems the bare harmonic-oscillator frequency Ω of the PQW, which is solely determined by the curvature of the confining potential, equals the plasma frequency of the three-dimensional electron gas which is a consequence of the generalized Kohn's theorem.[4]

Magnetotransport and far-infrared (FIR) investigations have uncovered a large amount of interesting results that shed some light onto the understanding of many fundamental properties of low-dimensional systems.[1–10] FIR spectroscopy on such structures yielded information of the generalized Kohn's theorem,[4] i.e., a perfect PQW absorbs far-infrared radiation at the bare harmonic-oscillator frequency Ω and is independent of the electron-electron interaction and the electron density in the well. Thus, it also has impact on the understanding of the infrared response of the harmonically bound quasi-one-dimensional quantum wires or quasi-zero-dimensional quantum dots, where the confining potentials in most cases can be regarded as parabolic. Theoretically, parabolic confining potentials are very attractive, since they allow many properties to be calculated in a rigorous and analytical fashion.

A powerful method to investigate the FIR magneto-optical properties of the electron gas in PQW is to use a tilted magnetic field that couples the in-plane motion of the carriers to the vertical one. This leads to an interaction between the cyclotron resonance ω_c and the harmonic oscillator Ω along the electric confining potential.

In the present paper, we will investigate the polaron effects due to the coupling of the electrons with longitudinal-optical (LO) phonon modes in a tilted magnetic field. The polaron energy levels will be calculated, and consequently, the cyclotron resonance transition energies are obtained. The influence of the direction of the magnetic field on the polaron effect as well as the possible magnetopolaron resonances will be studied.

Magnetopolaron effects in quasi-two-dimensional (Q2D) systems have been studied extensively in the last decade.[11–25] But almost all the work is based on the heterojunction and quantum well systems in the presence of a perpendicular magnetic field. Theoretically, only the Landau levels associated with the lowest electric subband were studied and a few papers involved in the polaron effects in PQW's. Larsen studied the polaron cyclotron frequency[13] within the Rayleigh-Schrödinger perturbation theory (RSPT), and the present authors calculated the polaron binding energy[26] in a PQW in the absence of any magnetic field. Later, Kühn and Selbmann investigated the magnetopolaron effects in a GaAs PQW (Ref. 23) and Haupt and Wendler[24] studied the effects of a tilted magnetic field on the polaron cyclotron mass. In the present paper, the magnetopolaron effects in the PQW's will be studied in tilted magnetic fields and beyond the lowest electric subband approximation. We will show the possible magnetopolaron resonances in higher energy regime.

The present paper is organized as follows. The Hamiltonian for the coupling of an electron to the LO phonons is given in Sec. II, and the bare electron states in a parabolic quantum well are also discussed. In Sec. III the polaron Landau levels in such a system will be calculated using degenerate second-order perturbation theory, from which we obtain the cyclotron frequency. We present our discussions and conclusions in Sec. IV.

II. THE HAMILTONIAN

We consider the coupling of an electron to the LO phonons in a parabolic quantum well structure in an arbitrary

 ©1999 The American Physical Society

magnetic field. The confinement potential is taken in the z-direction, and the two-dimensional (2D) electron gas is formed in the xy plane. A magnetic field $\mathbf{B} = (B\sin\theta, 0, B\cos\theta)$ is tilted over an angle θ with respect to the z axis. The system under consideration can be described by the Hamiltonian

$$H = H_e + H_{ph} + H_{ep} \tag{1}$$

with

$$H_e = \frac{p_x^2}{2m_b} + \frac{1}{2m_b}[p_y + eB(x\cos\theta - z\sin\theta)]^2 + \frac{p_z^2}{2m_b} + \frac{1}{2}m_b\Omega^2 z^2, \tag{2}$$

$$H_{ph} = \sum_{\vec{q}} \hbar\omega_{\rm LO}(b_{\vec{q}}^{\dagger} b_{\vec{q}} + \tfrac{1}{2}), \tag{3}$$

where $\vec{p}$ ($\vec{r}$) is the momentum (position) operator of the electron, m_b is the electron band mass, Ω is the harmonic-oscillator frequency of the parabolic quantum well, and $b_{\vec{q}}^{\dagger}$ ($b_{\vec{q}}$) is the creation (annihilation) operator of an optical phonon with wave vector $\vec{q}$ and energy $\hbar\omega_{\rm LO}$.

For an electron interacting with 3D bulk LO-phonon modes, the electron-phonon interaction Hamiltonian H_{ep} in Eq. (1) is given by the Fröhlich Hamiltonian

$$H_{ep} = \sum_{\vec{q}} (V_{\vec{q}} b_{\vec{q}} e^{i\vec{q}\cdot\vec{r}} + V_{\vec{q}}^{*} b_{\vec{q}}^{\dagger} e^{-i\vec{q}\cdot\vec{r}}), \tag{4}$$

where

$$V_{\vec{q}} = -i\hbar\omega_{\rm LO}\left(\frac{\hbar}{2m_b\omega_{\rm LO}}\right)^{1/4}\sqrt{\frac{4\pi\alpha}{Vq^2}}, \tag{5}$$

and α is the electron-phonon coupling constant. For polar semiconductors, such as GaAs and InAs, we have $\alpha \ll 1$, and consequently, we are allowed to use perturbation theory to incorporate the effect of the electron-phonon interaction on the electron energy levels. Thus, the electron states described by the Hamiltonian H_e are an essential ingredient in the calculation of the polaron effects within perturbation theory. In the following, we will give a short review of the bare electron states in the system.

First of all, let us consider the situation in which the magnetic field is perpendicular to the 2D electron gas plane, i.e., $\theta = 0$. In such a case, the z motion and the xy motion do not couple, and each electric subband has a set of Landau levels. The eigenenergy of the electron is given by

$$E^0_{m,n} = \hbar\Omega(m + \tfrac{1}{2}) + \hbar\omega_c(n + \tfrac{1}{2}), \tag{6}$$

where $m,n = 0,1,2,\ldots$ are the electric and the Landau-level indexes, respectively, and $\omega_c = eB/m_b$ is the unperturbed cyclotron frequency. The corresponding wave function can be written as

$$\Psi_{m,n,k_y}(x,y,z) = \phi_m(\Omega,z)\,\phi_n(\omega_c,\xi)\frac{1}{\sqrt{L_y}}e^{ik_y y} \tag{7a}$$

with

$$\phi_n(\omega,x) = \left(\frac{m_b\omega}{\pi\hbar}\right)^{1/4}\frac{1}{\sqrt{2^n n!}}H_n\left(\sqrt{\frac{m_b\omega}{\hbar}}x\right)\exp\left(\frac{-m_b\omega}{2\hbar}x^2\right), \tag{7b}$$

where $H_n(x)$ are the Hermite polynomials and $\xi = x + \hbar k_y/m_b\omega_c$.

When the magnetic field $\vec{B}$ is tilted away from the z direction, the electric and the magnetic quantizations are mixed. The Hamiltonian H_e can be diagonalized by a suitable rotation of the system with respect to the y axis. This leads to two decoupled harmonic oscillators in the new coordinate system (x',y,z') with frequencies[27]

$$\omega_{1,2} = \frac{1}{\sqrt{2}}(\omega_c^2 + \Omega^2 \pm \sqrt{\omega_c^4 + \Omega^4 - 2\omega_c^2\Omega^2\cos 2\theta})^{1/2}. \tag{8}$$

Notice that we defined $\omega_1 = \omega_+ > \omega_2 = \omega_-$. The electron energy is given by

$$E^0_{m,n} = \hbar\omega_1(m + \tfrac{1}{2}) + \hbar\omega_2(n + \tfrac{1}{2}), \tag{9}$$

where $m,n = 0,1,2,\ldots$. And the wave function

$$\Psi_{m,n,k_y}(x',y,z') = \phi_m(\omega_1,\eta')\,\phi_n(\omega_2,\xi')\frac{1}{\sqrt{L_y}}e^{ik_y y}, \tag{10}$$

where $\phi_n(\omega,x)$ is given by Eq. (7b), $\eta' = z' + \gamma_1\hbar k_y/m_b\omega_1$, $\xi' = x' + \gamma_2\hbar k_y/m_b\omega_2$,

$$\gamma_1 = \left(\frac{\omega_1^2 - \Omega^2}{\omega_1^2 - \omega_2^2}\right)^{1/2}, \tag{11a}$$

and

$$\gamma_2 = \left(\frac{\omega_1^2 - \omega_c^2}{\omega_1^2 - \omega_2^2}\right)^{1/2}. \tag{11b}$$

Notice that the level indexes m and n in Eq. (6) have a different meaning from those in Eq. (9). The former corresponds to Ω and ω_c, and the latter to ω_1 and ω_2. For the case of a tilted magnetic field, ω_2 is mainly determined by ω_c when $\omega_c < \Omega$ and ω_1 by Ω. For $\omega_c > \Omega$, the situation is the opposite, i.e., ω_1 is mainly determined by ω_c and ω_2 by Ω.

III. POLARON EFFECTS

In this section, we will calculate the magnetopolaron energy levels including the electron-LO-phonon coupling. Using second-order perturbation theory, the polaron energy in such a system can be written as

$$E_{m,n} = E^0_{m,n} + \Delta E_{m,n}, \tag{12}$$

where $\Delta E_{m,n}$ is the energy shift due to electron-phonon interaction, which is given by

$$\Delta E_{m,n}=-\sum_{m'=0}^{\infty}\sum_{n'=0}^{\infty}\sum_{\vec{q}}\frac{|M_{mn,m'n'}(\vec{q})|^2}{\hbar\omega_{\rm LO}-\Delta_{m,n}+E^0_{m',n'}-E^0_{m,n}}, \tag{13}$$

where $\Delta_{m,n}=\Delta E_{m,n}-\Delta E_{0,0}$ within the improved Wigner-Brillouin perturbation theory,[12,28] and

$$M_{mn,m'n'}(\vec{q})=\langle m',n';\vec{q}|H_{ep}|m,n;0\rangle \tag{14}$$

is the matrix element of the electron-phonon interaction H_{ep}, the ket $|n,l;\vec{q}\rangle=|n\rangle\otimes|l\rangle\otimes|\vec{q}\rangle$ describes a state composed of an electron in the level (m,n) and an optical phonon with momentum $\hbar\vec{q}$ and energy $\hbar\omega_{\rm LO}$.

For the case of $90°>\theta>0$, using Eqs. (4) and (10), the interaction matrix element in Eq. (14) reduces to

$$|M_{mm',nn'}(\vec{q})|^2=|V_q|^2G_{mm'}(\xi_1)G_{nn'}(\xi_2) \tag{15a}$$

with

$$G_{nn'}(\xi)=\frac{n_{\min}!}{n_{\max}!}\xi^{2(n_{\max}-n_{\max})}e^{-\xi^2}[L_{n_{\min}}^{n_{\max}-n_{\min}}(\xi^2)]^2, \tag{15b}$$

where $m_{\min}=\min(m,m')$, $m_{\max}=\max(m,m')$, $n_{\min}=\min(n,n')$, $n_{\max}=\max(n,n')$,

$$\xi_1^2=\hbar(q_{z'}^2+\gamma_1^2q_y^2)/2m_b\omega_1,$$

$$\xi_2^2=\hbar(q_{x'}^2+\gamma_2^2q_y^2)/2m_b\omega_2,$$

and $L_m^n(x)$ are the Laguerre polynomials.

Inserting Eq. (15) into Eq. (13), we obtain

$$\begin{aligned}\Delta E_{m,n}=&-\frac{2\alpha(\hbar\omega_{\rm LO})^2}{\pi\sqrt{\pi}}\sum_{m'=0}^{\infty}\sum_{n'=0}^{\infty}\frac{1}{\hbar\omega_{\rm LO}+E^0_{m',n'}-E^0_{m,n}-\Delta_{m,n}}\frac{m_{\min}!}{m_{\max}!}\frac{n_{\min}!}{n_{\max}!}\sum_{j=0}^{m_{\min}}\sum_{j'=0}^{m_{\min}}\frac{(-1)^{j+j'}}{j!j'!}\binom{m_{\max}}{m_{\min}-j}\\&\times\binom{m_{\max}}{m_{\min}-j'}\sum_{l=0}^{n_{\min}}\sum_{l'=0}^{n_{\min}}\frac{(-1)^{l+l'}}{l!l'!}\binom{n_{\max}}{n_{\min}-l}\binom{n_{\max}}{n_{\min}-l'}\frac{[2(M+N)-1]!!}{2^{M+N}}\\&\times\int_0^{x_0}dx\int_0^{\pi/2}d\theta\frac{\omega_1\omega_2}{\omega_1\omega_2-\omega_{\rm LO}[\omega_2(\gamma_1^2-\cos^2\theta)+\omega_1(\gamma_2^2-\sin^2\theta)]x^2}\left[\frac{\omega_2\cos^2\theta-(\gamma_2^2-\sin^2\theta)x^2}{\omega_2\cos^2\theta+\omega_1\sin^2\theta}\right]^M\\&\times\left[\frac{\omega_1\sin^2\theta-(\gamma_1^2-\cos^2\theta)x^2}{\omega_2\cos^2\theta+\omega_1\sin^2\theta}\right]^N,\end{aligned} \tag{16}$$

where $M=m_{\max}-m_{\min}+j+j'$, $N=n_{\max}-n_{\min}+l+l'$, and $x_0=\sqrt{\omega_1\omega_2/\omega_{\rm LO}(\gamma_1^2\omega_2+\gamma_2^2\omega_1)}$.

Equation (16) can be used to calculate the polaron energy $\Delta E_{m,n}$ numerically. But for small ω_c and Ω, the sum over n' and m' converge very slowly, and it is impossible to obtain the correct results for $\Delta E_{m,n}$. To avoid this defect, we follow Ref. 12 and cast the sum into an integration representation. For the energy below the LO phonon, i.e., $E<E_{0,0}+\hbar\omega_{\rm LO}$, $\Delta E_{m,n}$ becomes

$$\begin{aligned}\Delta E_{m,n}=&-\sum_{\vec{q}}|V_q|^2\int_0^{\infty}du\,e^{-(\hbar\omega_{\rm LO}-\Delta_{m,n})u}\\&\times\langle m,n|e^{i\vec{q}\cdot\vec{r}(u)}e^{-i\vec{q}\cdot\vec{r}(0)}|m,n\rangle,\end{aligned} \tag{17}$$

where $\vec{r}(u)$ is the electron position operator at imaginary time $u=it$ as described by the Hamiltonian without electron-phonon interaction. For real time, one has

$$x(t)=-\frac{\gamma_1\hbar k_y}{m_b\omega_1}+\sqrt{\frac{\hbar}{2m_b\omega_1}}(a^+e^{i\omega_1t}+a^-e^{-i\omega_1t}), \tag{18a}$$

$$\begin{aligned}y(t)=&-i\gamma_1\sqrt{\frac{\hbar}{2m_b\omega_1}}(a^+e^{i\omega_1t}-a^-e^{-i\omega_1t})\\&+\gamma_2\sqrt{\frac{\hbar}{2m_b\omega_2}}(c^+e^{i\omega_2t}-c^-e^{-i\omega_2t}),\end{aligned} \tag{18b}$$

$$z(t)=-\frac{\gamma_2\hbar k_y}{m_b\omega_2}+\sqrt{\frac{\hbar}{2m_b\omega_2}}(c^+e^{i\omega_2t}+c^-e^{-i\omega_2t}), \tag{18c}$$

where a^+ (a^-) and c^+ (c^-) are the creation (annihilation) operators for the states corresponding to the quantum numbers m and n, respectively. They are defined by

$$a^{\pm}=\sqrt{\frac{m_b\omega_1}{2\hbar}}\left(z'+\frac{\gamma_1}{m_b\omega_1}p_y\right)\mp i\frac{p_{z'}}{\sqrt{2\hbar m_b\omega_1}} \tag{19}$$

and

$$c^{\pm}=\sqrt{\frac{m_b\omega_2}{2\hbar}}\left(x'+\frac{\gamma_2}{m_b\omega_2}p_y\right)\mp i\frac{p_{x'}}{\sqrt{2\hbar m_b\omega_2}}, \tag{20}$$

and they satisfy the commutation relations $[a^-,a^+]=1$, $[c^-,c^+]=1$, and $[a^{\pm},c^{\pm}]=0$.

By using the above relations, we obtain the following representation for the energy shift due to the electron-phonon interaction

$$\Delta E_{m,n}=-\frac{\alpha\hbar\omega_{\rm LO}}{\sqrt{\pi}}\int_0^\infty du e^{-(1-\Delta_{m,n}/\hbar\omega_{\rm LO})u}$$
$$\times\sum_{m'=0}^{m}\binom{m}{m'}\frac{1}{m'}\left[\frac{4\omega_{\rm LO}}{\omega_1}\sinh^2\left(\frac{\omega_1 u}{2\omega_{\rm LO}}\right)\right]^{m'}$$
$$\times\sum_{n'=0}^{n}\binom{n}{n'}\frac{1}{n'}\left[\frac{4\omega_{\rm LO}}{\omega_2}\sinh^2\left(\frac{\omega_1 u}{2\omega_{\rm LO}}\right)\right]^{n'}P_{m',n'}(u), \tag{21a}$$

with

$$P_{m',n'}(u)=\frac{(-1)^{m'}(2(m'+n')-1)!!}{[2(\beta_2-\beta_1)]^{m'+n'}}\times\sum_{j=0}^{m'}\binom{m'}{j}\sum_{l=0}^{n'}\binom{n'}{l}\frac{\beta_1^l\beta_2^j}{\sqrt{\Lambda}}Q_{j+l}(u), \tag{21b}$$

where

$$Q_0(u)=\int_0^1 dt\frac{\Lambda}{\sqrt{[\Lambda-\gamma_1^2(\beta_1-\beta_2)t^2][\Lambda+\gamma_2^2(\beta_1-\beta_2)t^2]}} \tag{21c}$$

for $j+l=0$, and

$$Q_{l+j}(u)=\frac{(-1)^{l+j}}{\sqrt{\beta_1\beta_2}}\sum_{s=0}^{k+l-1}\binom{j+l-1}{s}\times\frac{[2(j+l-s-1)-1]!!s!}{[2(j+l)-1]!!\beta_1^s\Lambda^{j+l-s}}\times\sum_{r=0}^{s}\frac{[2(s-r)-1]!!(2r-1)!!}{(s-r)!r!}\left(\frac{\beta_1}{\beta_2}\right)^r \tag{21d}$$

for $j+l\geqslant 1$, where

$$\beta_1=\frac{\omega_{\rm LO}}{\omega_1}(1-e^{-\omega_1 u/\omega_{\rm LO}}), \tag{22a}$$

$$\beta_2=\frac{\omega_{\rm LO}}{\omega_2}(1-e^{-\omega_2 u/\omega_{\rm LO}}), \tag{22b}$$

and $\Lambda=\gamma_1^2\beta_1+\gamma_2^2\beta_2$.

When $\theta=0$, the magnetic field is perpendicular to the 2D electron gas. For this case, we performed a similar calculation, and we found that the above formulas (16) and (21) are still valid if we make the following substitution: $\omega_1\to\Omega$, $\omega_2\to\omega_c$, $\gamma_1\to 0$, $\gamma_2\to 1$,

$$\beta_1\to\beta_\Omega=\frac{\omega_{\rm LO}}{\Omega}(1-e^{-\Omega u/\omega_{\rm LO}}), \tag{23}$$

and

$$\beta_2\to\beta_{\omega_c}=\frac{\omega_{\rm LO}}{\omega_c}(1-e^{-\omega_c u/\omega_{\rm LO}}). \tag{24}$$

For $\theta=0$, we proved that the present calculation is able to recover: (i) the 3D result[12] when $\Omega\to 0$, (ii) the ideal 2D result[12] when $\Omega\to\infty$, (iii) the polaron binding energy in the absence of the magnetic field of Ref. 26 when $\omega_c\to 0$, and (iv) the shift of the cyclotron-resonance transition energy $\Delta E_{0,1}-\Delta E_{0,0}$ within RSPT as calculated in Ref. 13 when we take $\Delta_{1,0}=0$ in Eq. (13).

The polaron energy levels have been calculated as a function of the magnetic field ω_c. Figure 1 shows the polaron levels in a GaAs/Al$_x$Ga$_{1-x}$As PQW of $\Omega=0.7\omega_{\rm LO}$ for different orientations of the magnetic field: (a) $\theta=0$, (b) $\theta=15°$, (c) $\theta=45°$, and (d) $\theta=75°$. In the calculation, we took $\alpha=0.068$. The lower figures give the polaron energy levels of the series $m=0$, and $n=0$ (solid curves), $n=1$ (dashed curves), $n=2$ (dot-dashed curves), and $n=3$ (dotted curves). The upper figures give the levels of $m=1$, and $n=0$ (dashed curves), $n=1$ (dot-dashed curves), and $n=2$ (dotted curves). The thin solid curves are the unperturbed bare electron energies $E_{m,n}^0$, and the thin dotted curves are the energy levels $E_{m,n}^{\rm res}=E_{0,0}+m\hbar\omega_1+n\hbar\omega_2+\hbar\omega_{\rm LO}$. We found that the polaron effect: (1) shifts the energy levels to lower energy, (2) for $\theta=0$, the Landau levels split around $E_{m,n}^{\rm res}$ (the thin dotted curves) due to the magnetopolaron resonances, and (3) when the magnetic field is tilted away from the z direction, the electric and the magnetic quantizations are mixed. But the splitting of the energy levels still occurs around $E_{m,n}^{\rm res}$. Notice that the $E_{m,n}^{\rm res}$ depends on θ. It is seen that when $\theta>0$, e.g., $\theta=15°$, the left part of $\omega_c<\Omega=0.7\omega_{\rm LO}$ in Fig. 1(b) is similar to the corresponding part of that at $\theta=0$ in Fig. 1(a). But, when $\omega_c>\Omega=0.7\omega_{\rm LO}$, we also found that $E_{1,0}$ at $\theta=15°$ (the dashed curves) in the upper figure of Fig. 1(b) corresponds to $E_{0,1}$ at $\theta=0$ (the dashed curves) in the lower figure of the Fig. 1(a), and they have a similar magnetopolaron splitting behavior. In the case of $\theta=45°$ and 75°, the results are similar. For the higher energy levels, the situation becomes more complex because many resonances are found due to the strong mixing of the energy levels.

With increasing θ, ω_2 decreases, which is clearly apparent in Fig. 1(d) ($\theta=75°$) where the distance between the energy levels becomes very small. In this case, the energy levels above the LO-phonon continuum split into many sections due to the magnetopolaron resonances. In the limit of $\theta=90°$ all the levels with the same m are degenerate, and the upper and lower parts of the figures should collapse.

Next we consider the case of $\Omega>\omega_{\rm LO}$. Figure 2 shows the polaron levels in a PQW for $\Omega=1.4\omega_{\rm LO}$ with (a) $\theta=0$, (b) $\theta=15°$, (c) $\theta=45°$, and (d) $\theta=75°$. The polaron energy levels of $m=0$, and $n=0$ (solid curve), $n=1$ (dashed curves), $n=2$ (dot-dashed curves), and $n=3$ (dotted curves) are plotted in the lower part of the figures, and the levels of $m=1$, and $n=0$ (dashed curves), $n=1$ (dot-dashed curves), and $n=2$ (dotted curves) are given in the upper figures. The thin solid curves indicate the unperturbed electron energy levels $E_{m,n}^0$ and the thin dotted curves indicate the energies $E_{m,n}^{\rm res}=E_{0,0}+m\hbar\omega_1+n\hbar\omega_2+\hbar\omega_{\rm LO}$.

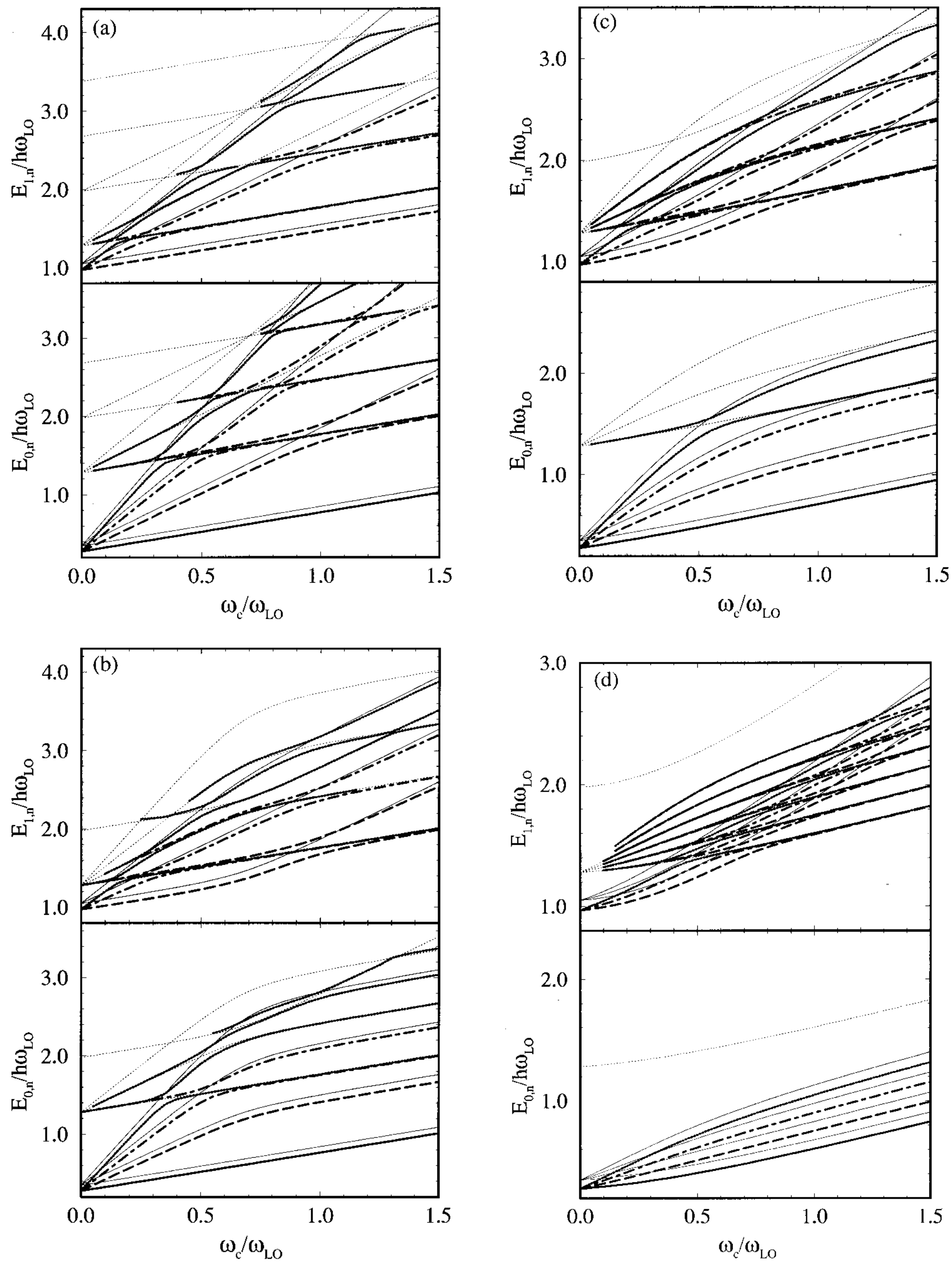

FIG. 1. The polaron energy levels in a parabolic quantum well with confinement frequency $\Omega=0.7\omega_{LO}$ for different magnetic field orientations: (a) $\theta=0$, (b) $\theta=15°$, (c) $\theta=45°$, and (d) $\theta=75°$. The lower figures give the levels of $m=0$, and $n=0$ (solid curve), $n=1$ (dashed curves), $n=2$ (dot-dashed curves), and $n=3$ (dotted curves). The upper figures give the levels of $m=1$, and $n=0$ (dashed curves), $n=1$ (dot-dashed curves), and $n=2$ (dotted curves). The thin solid curves indicate the unperturbed bare electron energy levels $E^0_{m,n}$, and the thin dotted curves indicate the energy levels $E_{0,0}+\hbar\omega_{LO}+m\hbar\omega_1+n\hbar\omega_2$.

Because $\Omega>\omega_{LO}$, the anticrossing of ω_1 and ω_2 occurs above the LO-phonon continuum $E_{0,0}+\hbar\omega_{LO}$. The splitting of the $E_{0,1}$ in Fig. 2(b) at $\theta=15°$ corresponds to that of the $E_{0,1}$ in Fig. 2(a) at $\theta=0$, which is different from that in Fig. 1 where $\Omega<\omega_{LO}$. But, in Figs. 2(c) and 2(d), this splitting is outside the calculated range ($\omega_c\leqslant1.5\omega_{LO}$).

For the higher energy levels $E_{1,n}$ in the upper figures, the results are quite different from those when $\Omega<\omega_{LO}$, especially for $\omega_c\ll\omega_{LO}$. In the upper figures of Fig. 2, we only give several branches. Actually, $E_{1,n}$ split into an infinitive number of branches according to perturbation theory so that it is impossible to obtain the exact positions of these levels at $\omega_c\to0$.

IV. DISCUSSIONS AND CONCLUSIONS

In a FIR magneto-optical spectroscopic investigation, the positions of the absorption peaks correspond to the transition energies between the above calculated energy levels. Some results have been obtained for magnetic field $B<12$ T in wide $Ga_{1-x}Al_xAs$ parabolic wells.[9]

In Fig. 3, the transition energies $E_{0,1}-E_{0,0}$ (thick solid curves) as well as $E_{1,0}-E_{0,0}$ (thick dashed curves) for a $\Omega=0.7\omega_{LO}$ PQW of GaAs are plotted as a function of the magnetic field for (a) $\theta=0$, (b) $\theta=15°$, (c) $\theta=45°$, and (d) $\theta=75°$. The energy difference between $E_{0,1}$ and $E_{0,0}$ ($E_{1,0}$ and $E_{0,0}$) is indicated by the thin solid (thin dashed) curves.

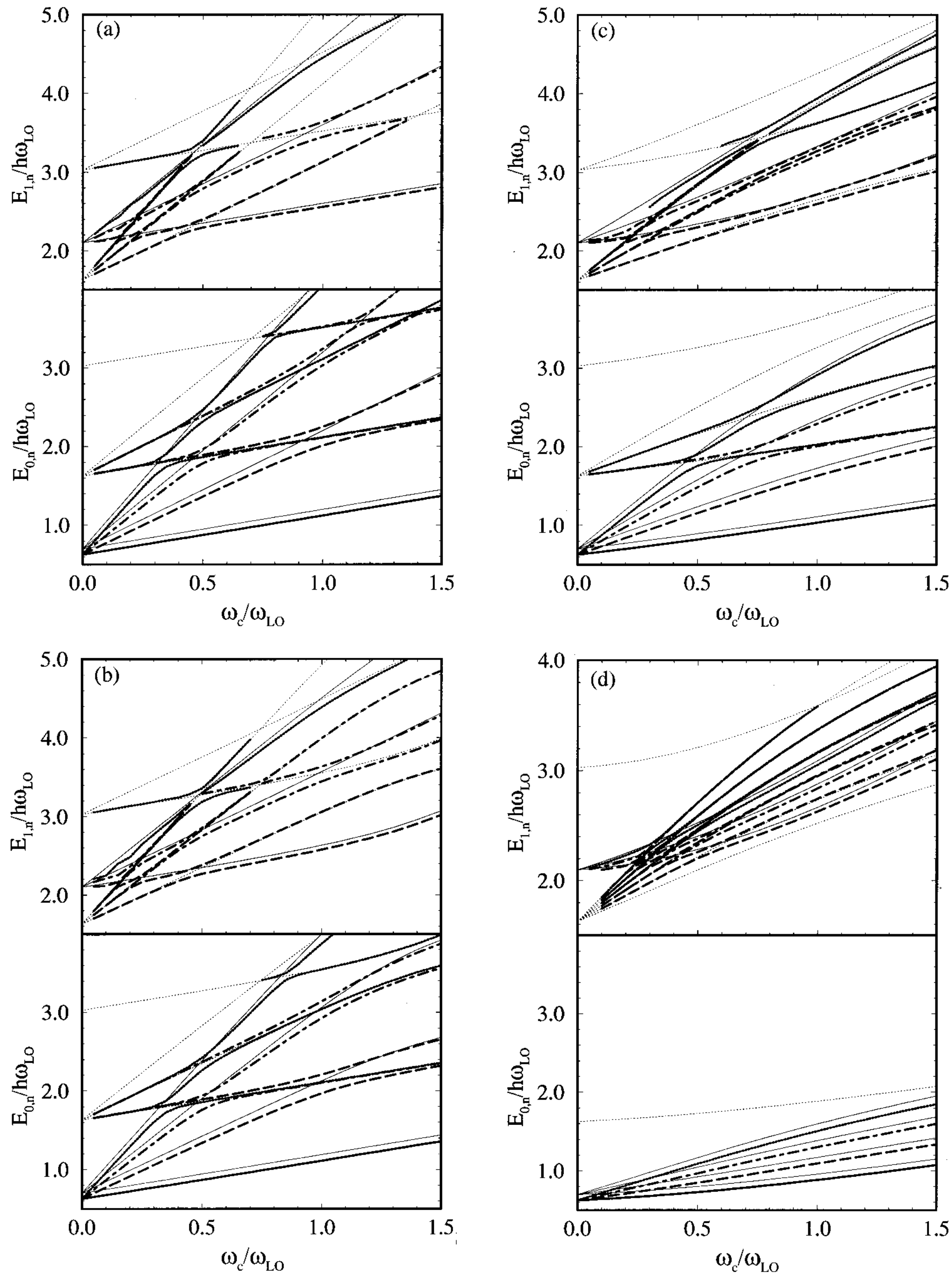

FIG. 2. The same as Fig. 1 but now for a parabolic well with $\Omega = 1.4\omega_{LO}$.

Notice that, at $\theta = 0$, the transition between two levels $E^0_{1,0}$ and $E^0_{0,0}$ in Fig. 3(a) is forbidden. We also find that the polaron correction to the ground state $E_{0,0}$ is smaller than that to the higher electric level $E_{1,0}$ as shown in Fig. 3(a). The difference between $\Delta E_{1,0}$ and $\Delta E_{0,0}$ is $0.012\hbar\omega_{LO}$ at zero magnetic field, and it decreases with increasing ω_c. The splitting around $\hbar\Omega$ results from the anticrossing of the ω_1 and ω_2, which increases with increasing θ. The other anticrossings occur for frequencies larger than $0.7\hbar\omega_{LO}$ and are a consequence of magnetopolaron resonances. We found that the position of the anticrossing near $\hbar\omega_{LO}$ decreases with increasing θ, and at the same time the splitting energy decreases. With increasing θ, more transitions become allowed just above the LO-phonon energy due to the magnetophonon effect, and the energy between them decreases.

In Fig. 4, we plot the transition energies $E_{0,1} - E_{0,0}$ and $E_{1,0} - E_{0,0}$ for $\Omega = 1.4\omega_{LO}$ PQW as a function of the magnetic field for (a) $\theta = 0$, (b) $\theta = 15°$, (c) $\theta = 45°$, and (d) $\theta = 75°$. We show that the transition between $E_{1,0}$ and $E_{0,0}$ can be strongly coupled with LO phonons when $\Omega > \omega_{LO}$ even for a perpendicular magnetic field ($\theta = 0$). This is significantly different from the case in which the transition energy is smaller than the phonon energy. For $\theta = 0°$ and 15°, such a coupling is pronounced in small magnetic fields, and results in the transition between $E_{1,0}$ and $E_{0,0}$ cannot be well defined when $\omega_c \to 0$. With increasing θ, the space between the levels of the splitted $E_{1,0}$ state decreases, and the electron-phonon coupling is enhanced as shown in Fig. 4(d).

In the case of a perpendicular magnetic field, one often defines the cyclotron mass $m^* = (\omega_c/\omega^*)m_b$, where ω^*

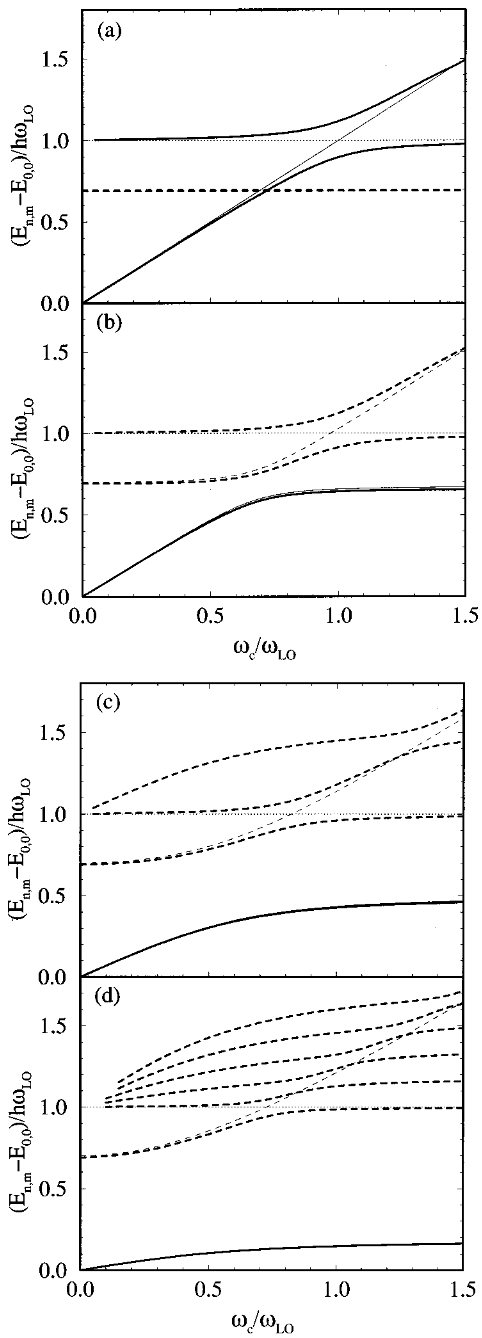

FIG. 3. The polaron transition energies $E_{0,1}-E_{0,0}$ (thick solid curves) and $E_{1,0}-E_{0,0}$ (thick dashed curves) as a function of magnetic field in a $\Omega=0.7\omega_{LO}$ parabolic well for (a) $\theta=0$, (b) $\theta=15°$, (c) $\theta=45°$, and (d) $\theta=75°$. The thin solid and thin dashed curves indicate the energy differences $E^0_{0,1}-E^0_{0,0}$ and $E^0_{1,0}-E^0_{0,0}$, respectively. The horizontal thin dotted line indicates the LO-phonon energy.

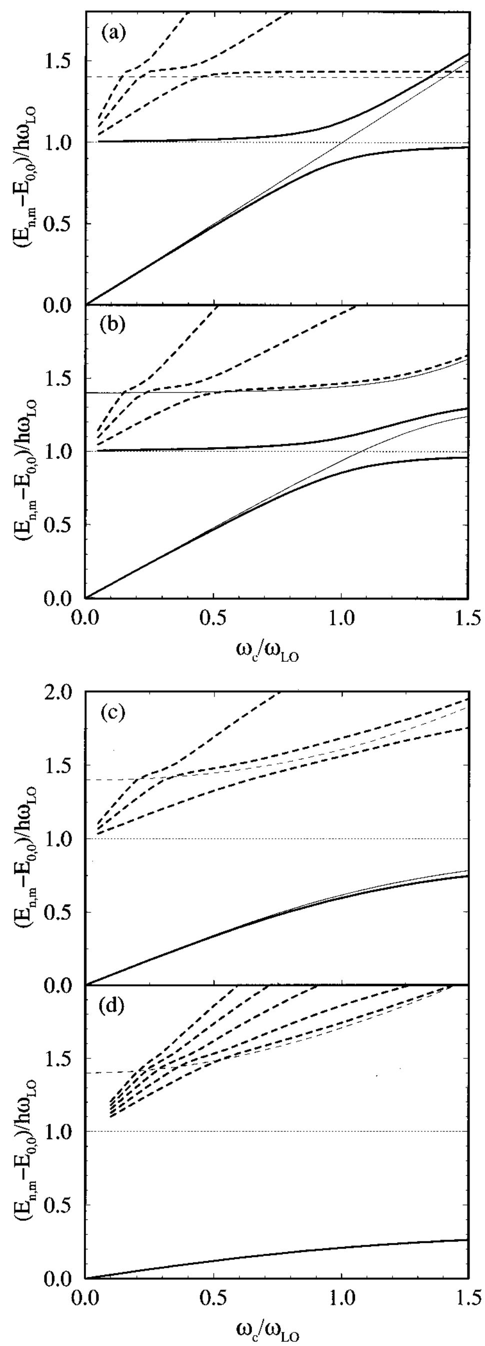

FIG. 4. The same as Fig. 3 but now for a parabolic well with $\Omega=1.4\omega_{LO}$.

$=(E_{0,1}-E_{0,0})/\hbar$ is the cyclotron frequency including the electron-phonon interaction, and $\omega_c=eB/m_b$ is the unperturbed cyclotron-resonance frequency. The polaron cyclotron mass is enhanced for $\omega^*<\omega_{LO}$ due to the electron-phonon coupling. By analogy with the perpendicular magnetic-field case, the authors of Refs. 23 and 24 defined the polaron cyclotron mass by $m^*/m_b=\hbar\omega_2/(E_{0,1}-E_{0,0})$ in the case of a tilted magnetic field. They calculated the lowest few polaron energy levels below the LO-phonon continuum and from which they obtained the polaron cyclotron mass. The present calculation is a generalization of the previous work and is valid for any Ω and ω_c. When $\Omega\to 0$ and $\Omega\to\infty$, the 3D and ideal 2D results can be recovered, respectively. While $\omega_c\to 0$, the result is also recovered in the absence of a magnetic field. As far as we know, the present paper presents the first study of the polaron effects of the higher subbands above the LO-phonon continuum in a Q2D system.

In conclusion, we have investigated the polaron effects of electrons coupled to the LO-phonon modes in parabolic quantum wells in the presence of a tilted magnetic field. The polaron energy levels are calculated within second-order perturbation theory in a multi-subband system. The influence of the direction of the magnetic field on the polaron effects was also studied. The magnetopolaron resonances occur at the energies $E^{\mathrm{res}}_{m,n}=E_{0,0}+m\hbar\omega_1+n\hbar\omega_2+\hbar\omega_{\mathrm{LO}}$ where a splitting of the polaron energy levels is found. Our calculation resulted in a very rich spectrum of polaron levels. When the unperturbed levels are higher than the energy $E_{0,0}+\hbar\omega_{\mathrm{LO}}$, it splits into an infinitive number of branches for $\omega_c\to 0$ but which carry negligible oscillator strength. It is expected that our results are also helpful to understand the magnetopolaron effects in other multisubband Q2D systems.

ACKNOWLEDGMENTS

This work was partially supported by CNPq, FAPESP (Brazil) and FWO, IUAP (Belgium). One of us (F.M.P.) is a Research Director with the Flemish Science Foundation (FWO).

[1] E. G. Gwinn, R. M. Westervelt, P. F. Hopkins, A. J. Rimberg, M. Sundaram, and A. .C. Gossard, Phys. Rev. B **39**, 6260 (1989).
[2] T. Sajoto, J. Jo, M. Santos, and M. Shayegen, Appl. Phys. Lett. **55**, 1430 (1989).
[3] K. Karrai, H. D. Drew, M. W. Lee, and M. Shayegan, Phys. Rev. B **39**, 1426 (1989).
[4] L. Brey, N. F. Johnson, and B. I. Halperin, Phys. Rev. B **40**, 10 647 (1989); F. M. Peeters, *ibid.* **42**, 1486 (1990).
[5] P. F. Hopkins, A. J. Rimberg, E. G. Gwinn, R. M. Westervelt, M. Sundaram, and A. C. Gossard, Appl. Phys. Lett. **57**, 2823 (1990).
[6] M. Kaloudis, K. Ensslin, A. Wixforth, M. Sundaram, J. H. English, and A. C. Gossard, Phys. Rev. B **46**, 12 469 (1992).
[7] V. Halonen, Phys. Rev. B **47**, 10 001 (1993).
[8] M. Zaluzny, Semicond. Sci. Technol. **6**, 112 (1991).
[9] A. Wixforth, Surf. Sci. **305**, 194 (1994).
[10] K. X. Guo and C. Y. Chen, J. Phys.: Condens. Matter **7**, 6583 (1995).
[11] J. T. Devreese and F. M. Peeters, in *The Physics of the Two-Dimensional Electron Gas*, edited by J. T. Devreese and F. M. Peeters (Plenum, New York, 1987), p. 131.
[12] F. M. Peeters and J. T. Devreese, Phys. Rev. B **31**, 3689 (1985).
[13] D. M. Larsen, Phys. Rev. B **30**, 4595 (1984).
[14] X.-G. Wu, F. M. Peeters, and J. T. Devreese, Phys. Rev. B **31**, 3420 (1985).
[15] X.-G. Wu, F. M. Peeters, and J. T. Devreese, Phys. Rev. B **34**, 8800 (1986).
[16] F. M. Peeters, X.-G. Wu, J. T. Devreese, C. J. G. M. Langerak, J. Singleton, D. J. Barnes, and R. J. Nicholas, Phys. Rev. B **45**, 4296 (1992).
[17] M. Horst, U. Merkt, and J. P. Kotthaus, Phys. Rev. Lett. **50**, 754 (1983).
[18] J. Scholz, F. Koch, J. Ziegler, and H. Maier, Solid State Commun. **46**, 665 (1983).
[19] M. Horst, U. Merkt, W. Zawadzki, J. C. Mann, and R. Ploog, Solid State Commun. **53**, 403 (1985).
[20] H. Sigg, P. Wyder, and J. A. A. J. Perenboom, Phys. Rev. B **31**, 5253 (1985).
[21] J. Singleton, R. J. Nicholas, D. C. Rogers, and C. T. B. Foxon, Surf. Sci. **196**, 429 (1988).
[22] G. Q. Hai, F. M. Peeters, and J. T. Devrees, Phys. Rev. B **47**, 10 358 (1993).
[23] O. Kühn and P. E. Selbmann, Semicond. Sci. Technol. **6**, 1181 (1992).
[24] R. Haupt and L. Wendler, Semicond. Sci. Technol. **9**, 803 (1994); Ann. Phys. (N.Y.) **214**, 233 (1994).
[25] K. Karraï, M. Stopa, X. Ying, H. D. Drew, and S. Das Sarma, Phys. Rev. B **42**, 9732 (1990).
[26] G. Q. Hai, F. M. Peeters, and J. T. Devreese, Phys. Rev. B **42**, 11 063 (1990).
[27] J. C. Maan, in *Two-Dimensional Systems, Heterostructures and Superlattices*, edited by G. Bauer, F. Kuchar, and H. Heinrich (Springer, Berlin, 1084), p. 183.
[28] G. Lindemann, R. Lasssnig, W. Seidenbusch, and E. Gornik, Phys. Rev. B **28**, 4693 (1983).